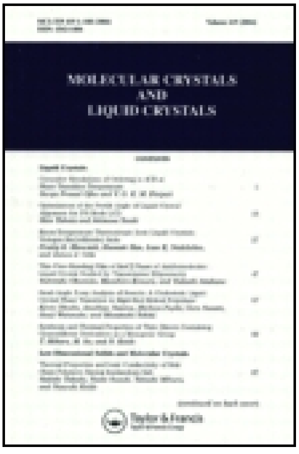

Molecular Crystals and Liquid Crystals
Publication details, including instructions for authors and subscription information:
http://www.tandfonline.com/loi/gmcl18

On the Fractal Distribution of Embryos at Nematic-Isotropic Critical Point

M. Nakagawa [a] , K. Kobayashi [a] , M. Hori [a] , M. Okabe [a] & Y. Hori [a]

[a] Department of Electrical Engineering, Faculty of Engineering, Nagaoka University of Technology, Kamitomioka 1603-1, Nagaoka, Niigata, 940-21, Japan
Version of record first published: 24 Sep 2006.

Mol. Cryst. Liq. Cryst., 1991, Vol. 195, pp. 15–26
Reprints available directly from the publisher
Photocopying permitted by license only

On the Fractal Distribution of Embryos at Nematic-Isotropic Critical Point

M. NAKAGAWA, K. KOBAYASHI, M. HORI, M. OKABE and Y. HORI

Department of Electrical Engineering, Faculty of Engineering, Nagaoka University of Technology, Kamitomioka 1603-1, Nagaoka, Niigata 940-21, Japan.

(Received November 10, 1989; in final form January 3, 1990)

In the present paper, a characteristic distribution of the nematic embryos of 5CB (4′-*n*-pentyl-4-cyanobiphenyls) is found to possess a statistically self-similar structure at the nematic-isotropic critical point. Three different measures, i.e., the covering measure, the entropy and the pair-correlation function between the embryos are evaluated to determine the fractal dimensionality. From the numerical processing, the fractal dimension D of the embryos floating in the isotropic sea, is evaluated as D ≃ 1.85 − 1.88, almost over 1 decade in scaling of space, evidently different from 2 for the randomly distributing, or spatially homogeneous case.

Keywords: fractals, nematic-isotropic critical point

1. INTRODUCTION

Since Mandelbrot founded a new modern geometry, i.e., fractals,[1] considerable attentions have been directed towards its comprehensive applicability to many scientific and engineering problems.[1–3] Especially, a generalization of the physical model for a fractional dimensionality of space is considered to be one of their attractive subjects. From such an apsect, recently, the critical phenomena on self-similar fratal lattices have been theoretically studied in connection with the renormalization- groups.[4–6] Especially it seems to be worthwhile to elucidate an inherent relationship between the fractal dimensionality D and the critical exponents in such model system.

The phase transitions of liquid crystals have been so far extensively investigated by many workers mainly based on the mean field approaches.[7–9] In such a mesogenic specimen one may see the intense light scattering near a clearing point because of the spatially distributing embryos, whose radii are comparable with the optical wave length, in the heterogeneous phase. Intuitively such embryos may be expected to be randomly distributed in the sample provided that the nuclei of the embryos are electrically neutral impurities floating in the mesogenic sea and have no interaction between them. On the other hand, the embryos may inhomogeneously distribute in space if there exists a certain correlation due to, e.g., such an electrostatic interaction as Coulomb force between them. In connection with this consideration, we may quote an experimental report by Nagaya *et al.* concerned with a phase separation process, whose time scale is of the order of 10 sec-10 min, in the 1:1 binary mixture of the polyethylene-terephtharate (PET) and a nematic liquid crystalline polymer (NLCP).[12] They observed that such a mixture first appears as a thread-like network and then changes to a cluster of the NLCP droplets with different sizes on the heating process after the temperature jump from the nematic phase to the isotropic one. In contradiction to the conclusion by Hasegawa *et al.*,[13] they concluded that there exists no self-similarity in the thread-like, or network, structure in the first time regime after the temperature jump from the nematic to the isotropic. Although they studied the spatial correlation of the network structure, they did not argue the spatial distribution of the nematic droplets of one component (NLCP) surrounded by the other component (PET). In analogous to their observation, even in a single component liquid crystal, a heterogeneous phase appears within very narrow temperature range of $\Delta T \sim 0.1 - 0.01$°C because such nematic-isotropic phase transitions are nearly second-order as is well-known.[7-9] Nevertheless it seems to be worthwhile to investigate the spatial distribution of the embryos in a single component nematic, which may be closely related to the spatial correlation of the nuclei at the clearing point and the interaction between embryos. As far as we are aware, however, there has been hitherto no report on the spatial distribution of the embryos at the clearing point of nematic liquid crystal.

From the above-mentioned respects, the present paper is addressed to a study of the spatial distribution of the nematic embryos appearing at the nematic-isotropic clearing point of 5CB on the cooling process. In §2 the experimental results will be presented and analyzed to evaluate the fractal dimensionalities specifying the spatial distribution of those nematic embryos. Finally §3 is devoted to several discussions and conclusions in connection with the size distribution of the presently observed embryos.

2. EXPERIMENTAL AND ANALYSIS

The nematic sample (5CB) was sandwiched between two bare glass plates separated from each other by 50μm with mylar spacers, and set in a thermostat whose temperature is accurately controlled within ±0.1°C by a micro-computer (PC8001mrkII:NEC) with a feed-back control circuit. Both surfaces of the glass plates were not chemically treated at all to avoid unfavourable anchoring effects on the nucleation of the nematic embryos. The sample was observed by an optical microscope with crossed polarizers (Optiphoto-pol:Nikon). For the illumination of the sample, a xenon stroboscopic flash (PS240:Sugawara) was used to obtain an enough exposure of the photographs in a short time because the nematic-isotropic transition of 5CB was quickly accomplished less than ~1 sec even with such a low cooling rate as 0.01°C/min in our observations. Although the sample temperature was well controlled of the order of $\Delta T \sim 0.01$ because the samples was sandwiched between the glass plates with a high thermal conductivity, we could not avoid the temperature inhomogeneity in the sample less than ~0.01°C at this stage from the structural geometry of the thermostat set to the optical microscope.

Figures 1(a)–(c) are the microscope photographs of the embryos appearing near

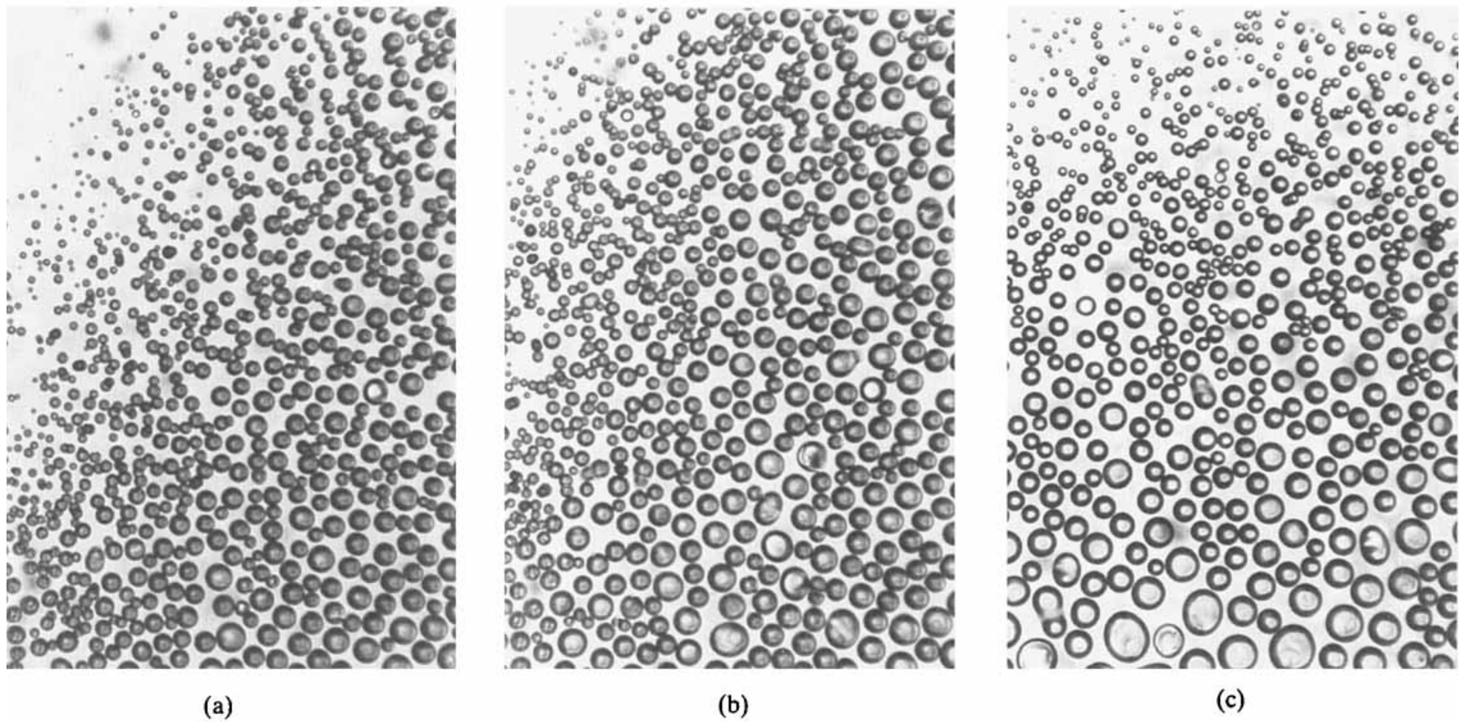

FIGURE 1 The photograph of the nematic embryos of 5CB at $T \simeq T_c$ (= 35.1°C). Here (a)–(c) were taken at a fixed position in the sample on three sequence of cooling processes. The cooling rate was set to about 0.01°C/min. See Color Plate I.

the critical point ($T \simeq T_c = 35.1°C$) on the cooling process from the isotropic liquid to the nematic phase. They show the same position in the sample. These embryos are in nematic phase with the optical birefringence, whereas the dark background is still in the isotropic phase. Therein the temperature of upper portion including relatively smaller embryos is slightly higher than that of the lower one. Of course such a temperature inhomogeneity in the sample is considered to be of the order of 0.01°C comparable with the coexistence temperature range of the single component nematics except for NLCP. We confirmed that the spatial positions of the embryos are fixed when they increase the sizes until they fuse into each other to make a larger droplet. It is noticeable here that these embryos are found to exclusively move each other when they increase their sizes. Therefore the large two embryos did not fuse into each other until at least one of them was captured by the anchoring force through the bounding plate. In Figure 1(a)–(c), most of embryos remained to be single as they grew up on the cooling process. At the present stage, we could not work with the time analysis of the evolution process of the embryos. This point will be reported in a separated paper in the near future. Since the typical size of the largest embryo in Figure 1(a)–(c) is almost the same as the sample thickness, those droplets may be virtually regarded as spheres floating in the isotropic sea. Next we picked up the spatial distribution of the centres of each embryos from Figure 1(a)–(c) by using a digitizer (MITABLET DT1000:Graphtech) with a resolution of 100μm. The total numbers of those points in Figure 1(a)–(c) were 941, 799, and 645 respectively. In what follows, let us evaluate the fractal dimensionality of the spatial distribution of these 2385 embryos by means of a few methods, using a micro-computer (PC-286VS:Epson), with the conventional least-square curve fitting. Especially, for the size distribution of these embryos, we shall mention in the next section.

First of all let us evaluate the capacity D_0 defined by[3,10]

$$D_0 = \frac{\Delta\,[\log\{n(R)\}]}{\Delta\,\{\log(1/R)\}}, \tag{1}$$

where R stands for the size of the $R \times R$ coarse-grained lattice, and $n(R)$ is the number of lattices which include at least one embryo in them. The plots of $\log\{n(R)\}$ vs $\log(1/R)$ are given in Figure 2. From the slope of that line determined by the least-square method, D_0 was evaluated as 1.86.

Next let us determine the information dimension D_1 defined by[3,10]

$$D_1 = \frac{\Delta\, I(R)}{\Delta\,\{\log(1/R)\}} = -\frac{\Delta[\sum_i p_i(R)\log\{p_i(R)\}]}{\Delta\{\log(1/R)\}}, \tag{2}$$

where $I(R)$ denotes the entropy of the spatial distribution of the embryos, $p_i(R)$ is the probability that the points are included in the ith coarse-grained lattice of size

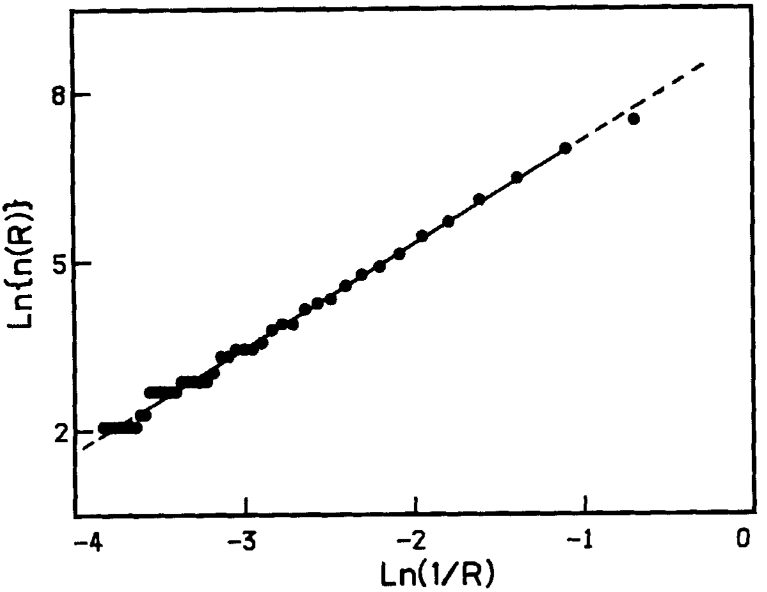

FIGURE 2 log{$n(R)$} − log($1/R$) plots for the capacity, D_0. Here the solid portion, almost over one decade, of the line corresponds to the part selected for the least-square method.

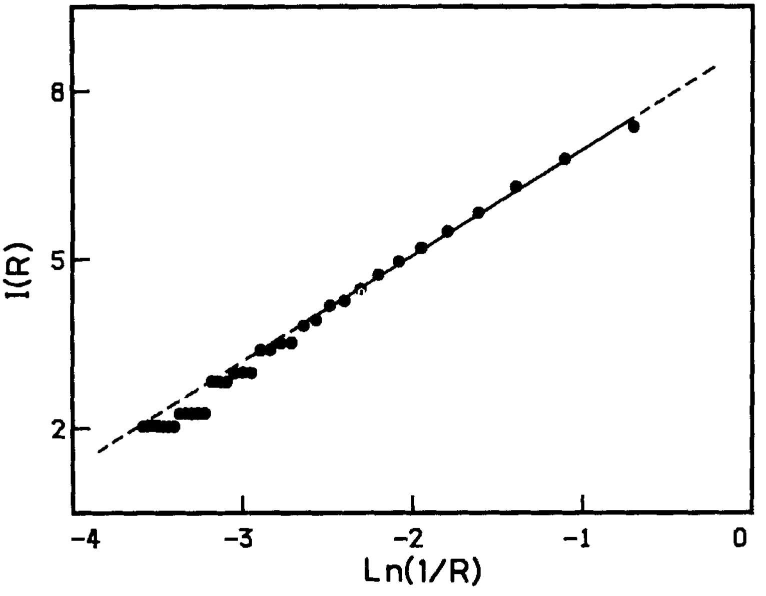

FIGURE 3 $I(R)$ − log($1/R$) plots for the information dimension, D_1. Here the solid portion, almost over one decade, of the line corresponds to the part selected for the least-square method.

$R \times R$, and the summation with respect to i ranges over all lattices. From Figure 3 D_1 was evaluated as 1.88.

Finally we shall evaluate the correlation dimension D_2 defined by[3,10]

$$D_2 = d - \frac{\Delta[\log\{g(r)\}]}{\Delta\{\log(1/r)\}}, \tag{3}$$

where $g(r) \propto 1/r^{d-D_2}$ is the pair correlation function between the embryos and assumed to be spatially isotropic, i.e., statistically independent of the direction of the relative position vector r between the embryos. From Figure 4 one obtains $D_1 \simeq 1.86$ in agreement with the aforementioned dimensionalities. At this stage, it may be noticeable here to examine the isotropy of the spatial correlation between the embryos. For this sake, let us first derive two dimensional correlation function $g(r)$ making use of the spectral density $S_{ff}(u)$ in the following manner,

$$\begin{aligned} g(r) &= \langle \delta(x)\delta(r+x) \rangle \\ &= \frac{1}{S}\int d^d x\, \delta(x)\delta(r+x) \\ &= \frac{1}{S}\int d^d u\, \exp(2\pi i u\cdot r)\, S_{ff}(u), \end{aligned} \tag{4}$$

$$S_{ff}(u) = |\Delta(u)|^2, \tag{5}$$

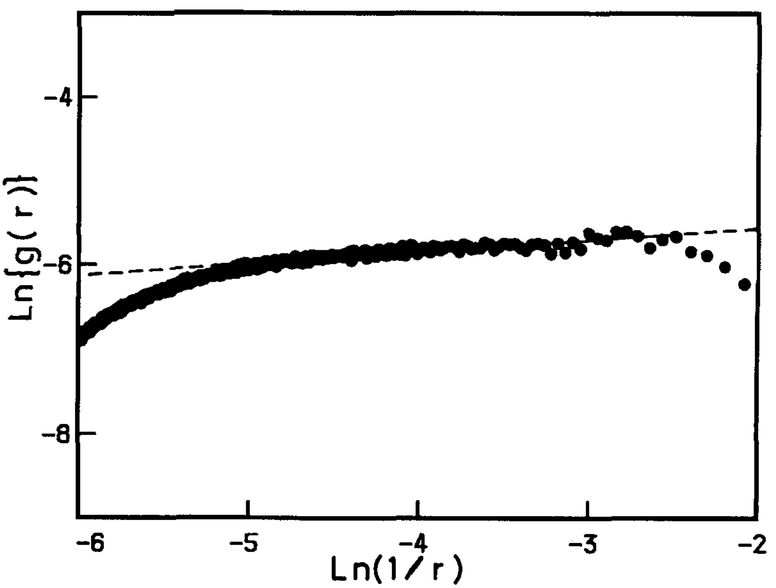

FIGURE 4 $\log\{g(r)\} - \log(1/r)$ plots for the correlation dimension, D_2. Here the solid portion, almost over one decade, of the line corresponds to the part selected for the least-square method.

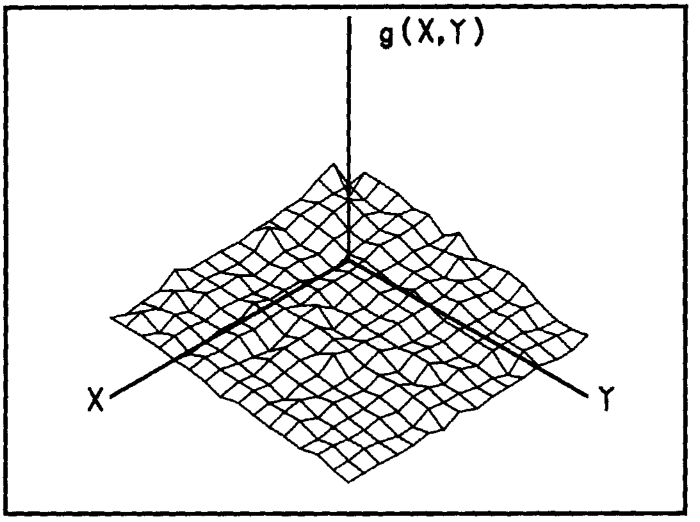

FIGURE 5 The two dimensional correlation function $g(X,Y)$ derived from Equations (4) and (6) to determine the correlation dimension and to confirm the isotropic correlation between the embryos.

$$\Delta(u) = \int d^d x \exp(-2\pi i u \cdot x)\delta(x), \tag{6}$$

where $\Delta(u)$ is the Fourier transform of $\delta(x)$, $2\pi u$ is the spatial wave vector, we replaced the ensemble average by the spatial one assuming the ergodicity with respect to the correlation function, S is the total area of the sample, and the occupation-function $\delta(r)$ is defined as

$$\delta(r) - \begin{cases} = 1 \text{ (if there exists an embryo at } r) \\ = 0 \text{ (otherwise).} \end{cases} \tag{7}$$

The conventional fast Fourier transform (FFT) program (128 × 128) was utilised to perform Equations (4) and (6) for the data of Figure 1(a) and (b). The resultant correlation function $g(r) = g(X,Y)$ is depicted in Figure 5, where the X axis corresponds to the horizontal direction in Figure 1(a)–(c), whereas the Y axis does to the vertical one. From $g(X,0)$ and $g(0,Y)$ shown in Figure 6(a) and (b), respectively, D_2 were evaluated as 1.87 and 1.85, respectively.

Summarising the above-mentioned results in Table I, the presently found fractal structure of the embryos at the critical point of 5CB may be specified by $D \simeq$ 1.85–1.88.

Evaluating the fractal dimensionality for the randomly distributed 2000 points distributing in the same area as Figure 1(a)–(c), we confirmed that $D \simeq 1.95$–1.99 almost equal to the Euclidean dimension $d = 2$.

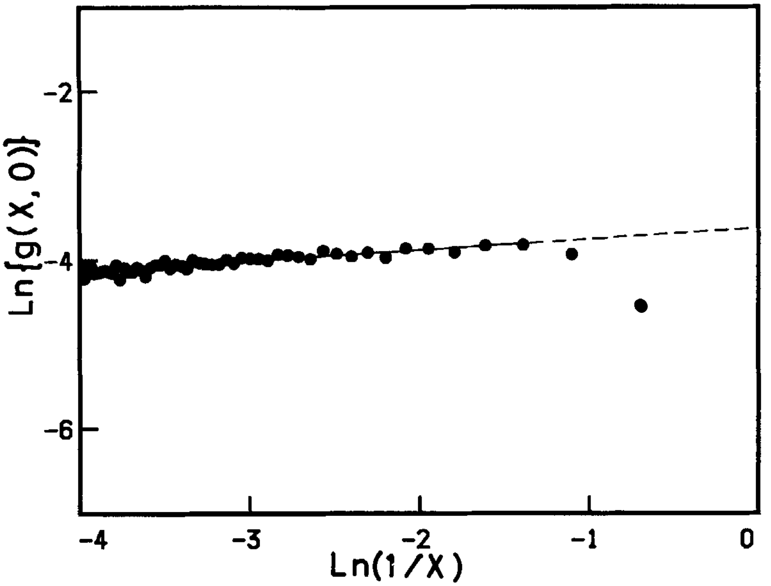

(a)

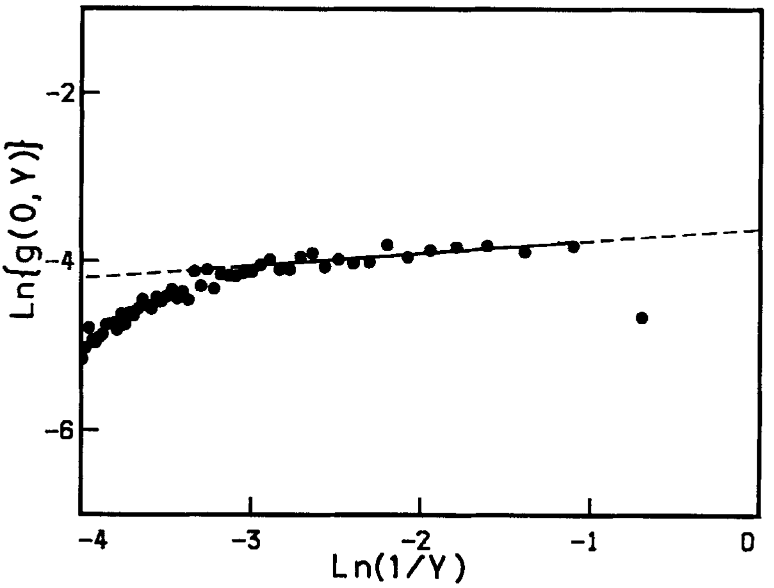

(b)

FIGURE 6 (a) log{$g(X,0)$} − log($1/X$) and (b) log{$g(0,Y)$} − log($1/Y$) plots corresponding to Figure 5.

Table I Fractal Dimensionalities for the nematic embryos

Capacity	Entropy	Correlation	2-dim Correlation using FFT(128×128)	
n(R)	I(R)	g(r)	g(X,0)	g(0,Y)
1.86	1.88	1.86	1.87	1.85

3. DISCUSSION AND CONCLUSION

In the present paper, we have investigated the spatial distribution of the nematic embryos at the nematic-isotropic clearing point. From the present analyses, the structure of the nematic embryos was found to be a statistically self-similar fractal characterised by $D \simeq 1.85-1.88$. This value just resembles that of the percolation clusters at the critical point reported by Peter *et al.*,[11] and is higher than 1.7 previously found in smectic focal domains.[10] This fact that the dimensionality D is significantly less than 2 (cf. Table I.) implies that the nuclei of the embryos floating in the isotropic phase are not independent of one another but certainly correlated probably through an electrostatic interaction as $\propto \sim 1/r^{3.4}$ according to the previous argument.[10] Obviously if they were generated independently in two dimensional space, the fractal dimensionality of the spatial distribution also has to lead to 2 as seen in the Brownian motion.[1,3] In other words, there may exist a certain interaction between the nuclei of the embryos in order that D is significantly less than 2 as was previously mentioned.

To conclude this study, let us mention below the size distribution of the presently found spherical embryos. For this sake, we first evaluated the probability density function $p(\mathbf{a})$ which is a measure of the number of embryos with the radii over $\mathbf{a} \sim \mathbf{a} + \Delta\mathbf{a}$. To examine whether the probability density function $p(\mathbf{a})$ follows such a scaling law as $p(\mathbf{a}) \propto 1/\mathbf{a}^{D+1}$ or not, let us introduce the probability function $P(\mathbf{a})$ defined by[3]

$$P(\mathbf{a}) = \int_{\mathbf{a}}^{\infty} d\mathbf{a}^* \, p(\mathbf{a}^*). \tag{8}$$

From $\log\{P(\mathbf{a})\}$ vs $\log(1/\mathbf{a})$ plots presented in Figure 7, one may see that $P(\mathbf{a})$ does not follow such a scaling law as $P(\mathbf{a}) \propto 1/\mathbf{a}^D$ in 1 decade of $\mathbf{a}$.[1,3] Hence one may conclude that there exists no relation between the size distribution and the spatial distribution for the presently found embryos in contrast to the case of the closely packed Apollonian disks.[1]

Alternatively let us attempt to interpret the functional form of $p(\mathbf{a})$ through the following argument. Here let σ be the interfacial energy per unit area between the nematic and the isotropic phases. Therefore, denoting the free energy densities in the isotropic and nematic phases as F_I and F_N, respectively, and ignoring the elastic energy due to the director field in the spherical embryo because of the low ori-

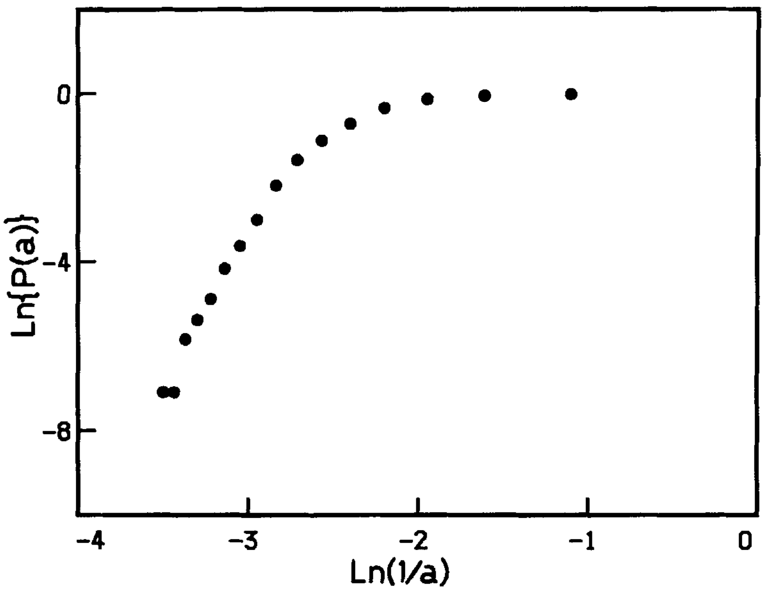

FIGURE 7 log{$P(\mathbf{a})$} − log(1/a) plots for the size distribution. Here $P(\mathbf{a})$ is the probability of the embryos whose radii are larger than **a**. If the size distribution follows such a power law as $P(\mathbf{a}) \propto 1/\mathbf{a}^D$, the slope of these plots will give the fractal dimension.

entational order of molecules, the nucleation energy of a single nematic embryo with the radius **a** in the isotropic phase, $\Phi(\mathbf{a})$, can be now written as

$$\Phi(\mathbf{a}) = \frac{4\pi}{3}\mathbf{a}^3 (F_N - F_I) + 4\pi\mathbf{a}^2\sigma. \tag{9}$$

Then, near the clearing point, the first term in the right-hand side may be discarded in comparison with the second term contribution. Hence it is natural to expect that $p(\mathbf{a})$ follows the following Gaussian distribution function,

$$\begin{aligned} p(\mathbf{a}) &\propto \exp(-\Phi(\mathbf{a})/k_B T_c) \\ &\sim \exp(-4\pi\mathbf{a}^2\sigma/k_B T_c), \end{aligned} \tag{10}$$

where k_B is the Boltzmann constant. To show the validity of the present argument, log{$p(\mathbf{a})$} vs $\mathbf{a}^2$ plots are given in Figure 8. Comparing it with Figure 7, it is plausible to say that $p(\mathbf{a})$ follows the Gaussian distribution rather than the power law as $1/\mathbf{a}^{D+1}$.

As a future problem, it seems to be significant to investigate systematically universality of the fractal dimension of the embryos at critical points for several kinds of liquid crystalline materials as well as the previously noted time evolution process of the embryos.

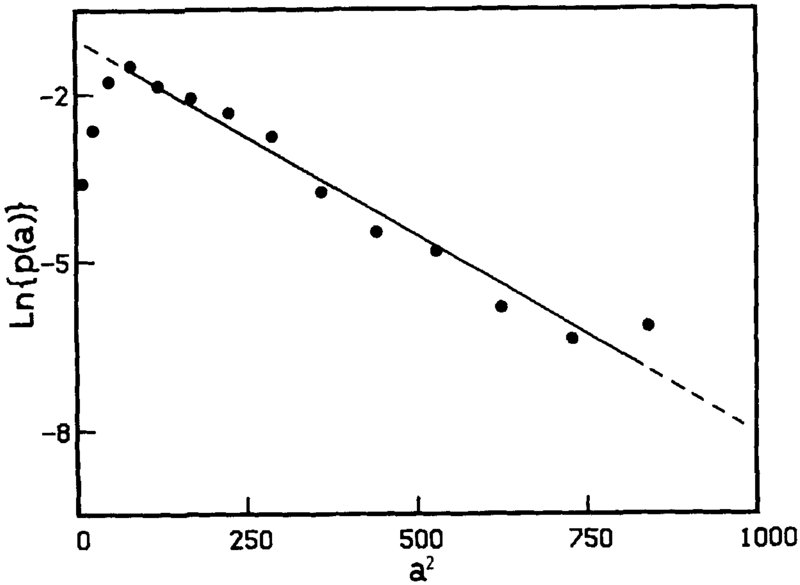

FIGURE 8 log{p(**a**)} – $\mathbf{a}^2$ plots for the size distribution. Here $p(\mathbf{a})$ is the probability density function of the embryos whose radii correspond to $\mathbf{a} \sim \mathbf{a} + \Delta\mathbf{a}$.

Acknowledgment

The present authors would like to express their thanks to Professor Tadashi Akahane and Mr. Kazuo Koyama at our university for the collaborations on the present experimental works.

References

1. B. B. Mandelbrot, *The Fractal Geometry of Nature*, (W. H. Freeman and Company, New York, 1982) Chap. 6.
2. *Fractals*: J. Feder (Plenum Press, 1988).
3. H. Takayasu, *Fractals* (Asakura Syoten, Tokyo, 1986), (in Japanese).
4. Y. Gefen, B. B. Mandelbrot and A. Aharony, *Phys. Rev. Lett.*, **45**, 855 (1980).
5. Y. Gefen, A. Aharony, Y. Shapir and B. B. Mandelbrot, *J. Phys.*, **A17**, 435 (1984).
6. T. Abe, *J. Phys. Soc. Jpn.*, **58**, 1962 (1989).
7. P. G. de Gennes, *The Physics of Liquid Crystals*, (Oxford Univ. Press, 1974), Chap. 2.
8. S. Chandrasekhar, *Liquid Crystals*, (Cambridge Univ. Press, 1977), Chap. 2.
9. G. Vertogen and W. H. de Jeu, *Thermotropic Liquid Crystals*, (Springer-Verlag, 1988), Part IV.
10. M. Nakagawa, *Jpn. J. Appl. Phys.*, **28**, 1636 (1989).
11. H. P. Peters, *et al.*, *Z. Physik.*, **B34**, 399 (1979).
12. T. Nagaya, H. Orihara and Y. Ishibashi, *J. Phys. Soc. Jpn.*, **58**, 3600 (1989).
13. H. Hasegawa, T. Shiwaku, A. Nakai and T. Hashimoto, in *Dynamics of Ordering Process in Condensed Matter* (S. Komura, ed.), (Plenum Press, 1988). p. 457.